Journal of Chromatography, 647 (1993) 3–12
Elsevier Science Publishers B.V., Amsterdam

CHROMSYMP. 2804

Peptide mapping of recombinant human interferon-γ by reversed-phase liquid chromatography with on-line identification by thermospray mass spectrometry and UV absorption spectrometry

Raymond Legrand, Jean-Bernard Falconnet☆, Daniele Prevost, Bernard Schoot and Philippe Devaux*

Physics Department, Roussel Uclaf Research Centre, 102 Route de Noisy, F-93230 Romainville (France)

ABSTRACT

The detection and identification of minor peaks in a complex peptide map of recombinant human interferon-γ was realized by on-line analysis of the eluted peptides using thermospray mass spectrometry and UV absorbance spectrometry. By this procedure the time-consuming process of collection, purification and chemical sequence analysis is avoided. Owing to the formation of multiply charged ions, the domain of the covered masses is extended. Fragmentation of the peptides in the thermospray source was observed resulting from, amongst others, cleavage by acid hydrolysis of peptide bonds involving an aspartic acid. This was of great use for the identification of peptides in a digest of recombinant human interferon-γ by *Staphylococcus aureus* strain V8 endoprotease.

INTRODUCTION

Peptide mapping is a widely used technique in the identification of proteins. It allows the identification and localization of a single amino acid substitution or its deletion in a protein and, therefore, it is a powerful method for checking the integrity of the molecule [1,2]. Changes in the structure of the molecule may be detected by the appearance of new peaks in RP-HPLC of the protein digest. After separation, the peptides have to be identified, in general, by an N-terminal sequence determination. Mass spectrometry and UV absorbance spectrometry are also of interest. Submicrogram amounts of material eluted from the LC column can be analysed by both methods. Mass spectrometry has become a valuable tool for peptide and protein analysis as it can provide accurate molecular mass and sequence information below the nanomole level [3].

To avoid lengthy sample clean-up procedures, on-line coupling of HPLC to mass spectrometry has been investigated for many years. Several interfaces have been described and are now routinely used: continuous-flow fast atom bombardment (FAB) [4,5], frit FAB [6,7], ionspray [8,9] and thermospray (TSP) [10–16]. It has been shown that thermospray ionization can generate multiply charged ions from peptides [12–14,17,18], thereby extending the mass range of a quadrupole instrument.

We report here the first application of LC–thermospray MS and HPLC–photodiode-array detection to the peptide mapping recombinant human interferon-γ (rhIFN-γ). In the course of this study, spontaneous fragmentation of peptides in the thermospray device was observed.

* Corresponding author.
☆ Present address: Hopital Debrousse, Service de Biochimie, 29 Rue Soeur Bouvier, F-69005 Lyon, France.

EXPERIMENTAL

Chemicals

rhIFN-γ (RU 42369) is extracted from *Escherichia coli*, into which a plasmid coding for this protein has been transfected. rhIFN-γ contains the sequence of 143 amino acids, as found in the natural protein, with the addition of an additional N-terminal methionine. This recombinant protein is not glycosylated.

Protease from *Staphylococcus aureus* strain V8 is an endoprotease, which hydrolyses peptide bonds specifically at the carboxylic side of glutamic acid (pH of incubation about 4.5 or 7) and aspartic acid (pH of incubation about 7.5). The enzyme preparation used for this study was purchased from Boehringer (Mannheim, Germany).

Acetonitrile and glacial acetic acid were purchased from E. Merck (Darmstadt, Germany). Trifluoracetic acid (TFA) (sequence grade) was from Pierce. Water was obtained from a Millipore (France) Milli-Q filtration unit.

Materials

The separation of the peptides by HPLC was performed using a Model 600 low-pressure gradient HPLC pump system (Waters–Millipore) equipped with a Rheodyne Model 7010/7012 manual injector.

Separation was carried out on a Beckman Ultrasphere C_{18} column (750 mm × 4 mm I.D.) packed with 3-μm particles.

The elution profile of the peptides was recorded by means of a Waters–Millipore Model 990+ diode-array detector system. The detector was equipped with a special high-pressure-resistant cell, in order to permit on-line coupling with a thermospray mass spectrometer. The chromatograms were analysed using the program accompanying the detector.

Acetic acid solution (16%, v/v) was delivered by means of a Waters M45 HPLC pump.

Mass spectrometry

All experiments were carried out on a Finnigan Model 4600 GC–LC–MS quadrupole mass spectrometer (mass range 1800 u) equipped with a slightly modified TSP-I thermospray ionization source (Finnigan-MAT, San Jose, CA, USA).

The standard planar repeller electrode of the Finnigan thermospray source was modified by sealing the filament electron aperture and by using a needle repeller electrode placed very near the sampling cone orifice as described by Robins and Crow [19]. This modification improves the sensitivity at higher masses and the stability of the ion current.

The vaporizer consists of a length of 0.007 in. I.D. syringe tubing (1 in. = 2.54 cm), tipped with a sapphire orifice that has a nominal orifice of 0.0026 in. (Finnigan TSP II). The mass spectrometer was calibrated in the electron impact (EI) mode using TRZ9 [tris(perfluorononyl)-*s*-triazine] and alternatively in the TSP mode with polyethylene glycol. Initial tuning of the instrument was carried out by infusion of a dilute solution of a peptide mixture of Leu-enkephalin, angiotensin, gramicidine S and IFN 10–38 (peptide of rhIFN-γ), concentration 10 μ*M* each, in water–acetonitrile–acetic acid (67:29:4, v/v/v).

Typical operating conditions were as follows: jet (source block) temperature, 230°C; vaporizer temperature, 75–80°C; repeller voltage, 30 V; mass spectrometer high vacuum, $4.0 \cdot 10^{-5}$ Torr (1 Torr = 133.322 Pa); and flow-rate, 1.5 ml/min. Data were collected over the mass range of interest using 4-s scans in the centroid mode.

Methods

Hydrolysis. Limited digestion of rhIFN-γ (1 mg/ml) with endoprotease from *Staphylococcus aureus* at an enzyme-to-IFN-γ ratio of 1:50 (w/w) was performed in 50 m*M* Tris–HCl buffer (pH 7.0) for 15 h at 37°C.

HPLC. A 200-μg amount of the hydrolysed protein was injected directly on to the HPLC column. The peptides were eluted with a gradient of 0.1% TFA in acetonitrile (B) and 0.1% TFA in distilled water (A), as follows: Initial, 100% A; 0–40 min, linear gradient from 0 to 20% (v/v) B in A; 40–60 min, linear gradient from 20 to 40% (v/v) B in A; 60–65 min, linear gradient from 40 to 50% (v/v) B in A; and 65–70 min, linear gradient from 50 to 0% (v/v) B in A. A 10-min delay was allowed before reinjection. The flow-rate was 1.2 ml/min.

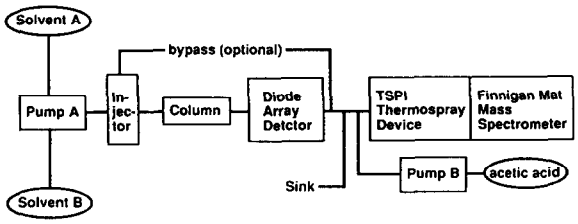

Fig. 1. Experimental set-up of the on-line RP-HPLC–diode-array UV detector–thermospray mass spectrometer system. Pump A, Waters Model 600 gradient pump; pump B, Waters M45 HPLC pump.

Spectra of the eluate in the wavelength range 220–290 nm were recorded at given intervals (about 1 s).

A solution of 16% (v/v) acetic acid in water was added at a flow-rate of 0.3 ml/min between the absorbance detector and the thermospray vaporizer.

The eluate was directed to waste during the 5 min immediately after injection of the sample, without passing through the thermospray ionizer, in order to prevent blockage by inorganic salt deposits. A schematic diagram of the experimental set-up is shown in Fig. 1.

RESULTS AND DISCUSSION

A typical peptide map obtained under the experimental conditions described above is shown in Fig. 2. The elution profile of the proteolytic digest is represented for the two modes of detection: total ion current from the mass spectrometer (Fig. 2b) and UV absorbance at 220 nm from the diode-array detector (Fig. 2a).

Two conclusions can be drawn from these chromatograms: first, the thermospray interface does not seem to affect the chromatographic resolution too dramatically, and second, if we consider that the absorbance at 220 nm is roughly proportional to the amount of material eluted from the column, it appears that the ionization efficiency by thermospray varies dramatically with the structure of the peptides, as the peak intensities given by the two detection modes are very different.

The results were analysed in the following way. For the absorbance profile, the absorption spectra between 240 and 290 nm of the peaks detected at 220 nm were analysed in the presence of phenylalanine (absorbance maximum at 250–260 nm), tyrosine (absorbance maximum at 280 nm, low absorbance at 290 nm) and tryptophan (absorbance maximum at 280 nm and relatively high absorbance at 290 nm). An example is given in Fig. 3, which represents the elution of the first peaks of the peptide map (peaks 1–6) together with the UV spectrum of each peak. The presence of an aromatic side-chain in peptides 3, 5 and 6, tryptophan, phenylalanine and tyrosine, respectively, was then concluded.

For the mass spectrometry profile, the 42 fractions numbered in Fig. 2b were analysed for the presence of fragments (peptides) in the mass range 300–1800 u. A search was made for each fraction to locate the amino acid sequence in rhIFN-γ that matches the observed mass, the absorption spectrum and with a C-terminal amino acid residue consistent with the specificity of the protease.

Table I summarizes the experimental data and the main conclusions in terms of identification of the peptides. All the peaks of the chromatogram were analysed in the same way. The retention time, the surface, the percentage of the total surface, the observed and theoretical mass, the proposed sequence and the nature of the UV chromophore of the peptide are given for each peak. The fragments printed in bold are characterized unambiguously as the parent fragments of a series. Sequences are coded by two numbers. The numbering is made according to the order of the first and the last amino acid of the peptide in the sequence of rhIFN-γ, assigning position 0 to the N-terminal methionine (this amino acid is absent in natural interferon gamma).

The amino acid sequence of rhIFN-γ is given in Fig. 4. The observed cleavage sites for *Staphylococcus aureus* strain V8 endoprotease are indicated.

Formation of multiply charged ions

The addition of acetic acid to the eluate after the diode-array detector (see Fig. 1) facilitates the ionization and in many instances the forma-

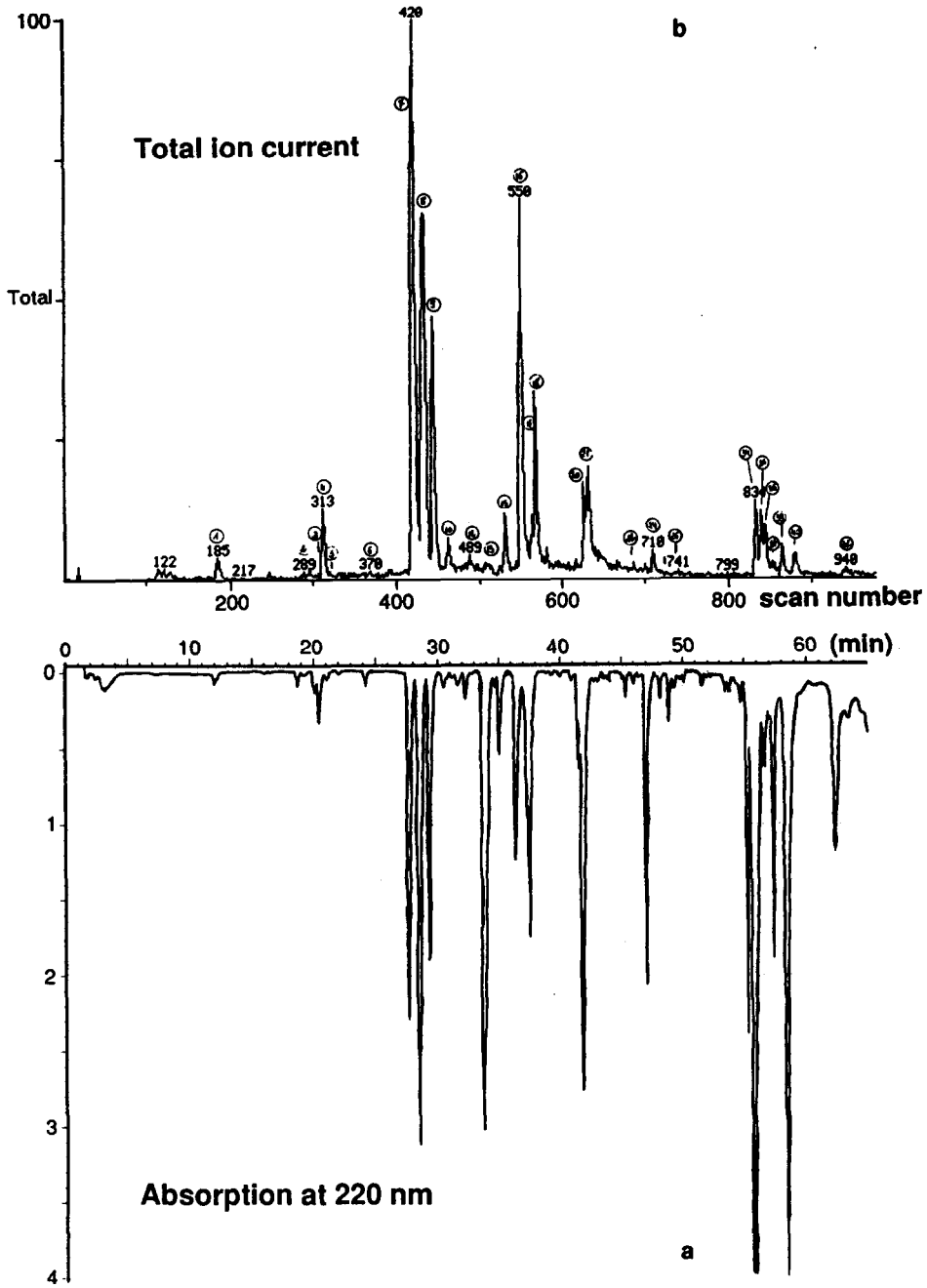

Fig. 2. Peptide map of rhIFN-γ. (a) Detection by UV absorbance at 220 nm; (b) detection by total ion current.

tion of multiply charged ions [17]. This extends the analytical power of the mass detector to peptides with masses over 1800 u and occasionally provides confirmation of sequence assignments for fragments appearing as several multiply charged ions in the spectra.

In this study we observed that direct thermospray ionization can generate multiply charged ions from the intact molecule for peptides of masses up to 3900 u. These multiply charged ions are represented in Table I. The presence of multiply charged ions was confirmed by the

TABLE I

ANALYSIS OF THE PEPTIDE OF rhIFN-γ HYDROLYZED BY *STAPHYLOCOCCUS AUREUS* STRAIN V8 ENDOPROTEASE IN Tris BUFFER, pH 7.0

200 μg hydrolyzate analyzed.

Retention time (min)	Surface (220 nm)[a]	% of total surface	Masses found $(M+xH)^{x+}$	Fragments identified	(M + H), theoretical	UV Spectrum
11.96 (peak 1)	2 581	0.2	490^{+}	**72–75**	489.6	No aromatics
18.71 (peak 2)	1 933	0.2	765^{2+}	**120–133**	1527.8	No aromatics
20.08 (peak 3)	3 740	0.3	705^{+} 912	35–39	704.7	Trp
20.44 (peak 4)	9 163	0.7	338^{2+}, 675^{+} 439^{2+}, 877^{+}	**42–46** **40–46**	674.9 877.0	No aromatics
21.07 (peak 5)	1 950	0.2	902^{+} 1748	77–83	899.1	Phe
24.22 (peak 6)	2 796	0.2	409^{+} 635^{+}	0–20X 3–7	408.0 634.7	Tyr
27.60 (peak 7)	74 555	5.9	605^{2+}, 1207^{+}	**103–112**	1207.4	No aromatics
28.44 (peak 8)	102 199	8.1	393^{+} 635^{+} 505^{2+}, 1009^{+}	0–2 3–7 **0–7**	392.4 634.7 1009.1	Tyr
29.28 (peak 9)	54 048	4.3	463^{2+}, 925^{+} 521^{2+}, 1040^{+}	94–101 **94–102**	925.0 1040.1	Tyr
30.46 (peak 10)	3 481	0.3	611^{2+}	**134–143**	1221.4	Phe
31.62 (peak 11)	4 046	0.3				Phe
32.27 (peak 12)	3 561	0.3	448 747 1126 1396 530^{2+}, 1059^{+}			Trp
33.68 (peak 13)	135 912	10.7	949 683^{4+}, 911^{3+}	 **120–143**	 2731.2	Phe
35.06 (peak 15)	14 472	1.1	640^{2+}, 1278^{+} 697^{2+}, 1393^{+}	10–20 **10–21**	1278.4 1393.5	Tyr
36.39 (peak 16)	40 921	3.2	804^{+}	**113–119**	803.0	No aromatics
37.30 (peak 17)	21 398	1.7	659^{2+}, 1317^{+} $869^{2+}/879^{2+}$ $927^{2+}/935^{2+}$ $985^{2+}/992^{2+}$ 1201^{+}	**92–102** 77–90 76–90 **76–91** 92–101	1316.4 1756.1 1871.1 1986.2 1201.3	Phe
37.55 (peak 18)	52 328	4.1	688^{2+}, 1375^{+} 782^{2+} 840^{2+}	10–21[b] 10–23 **10–24**	1393.5 1563.7 1678.8	Tyr
41.46 (peak 20)	11.461	0.9	$1022^{+}/1040^{+}$ 604^{2+}, 1208^{+} 744^{3+}, 1115^{2+}	94–102 103–112 **94–112**	1040.1 1207.4 2229.5	Tyr
41.75 (peak 21)	108 336	8.6	410^{+} $869^{2+}/877^{2+}$ $927^{2+}/936^{2+}$ 985^{2+} 1074^{2+} 754^{3+}, $1123^{2+}/1132^{2+}$ 975 998	91–93 77–90 76–90 76–91[b] 77–93 **76–93**	409.4 1756.1 1871.1 1986.2 2147.4 2262.5	Phe

(*Continued on p. 8*)

TABLE I *(continued)*

Retention time (min)	Surface (220 nm)[a]	% of total surface	Masses found $(M+xH)^{x+}$	Fragments identified	(M + H), theoretical	UV Spectrum
45.38 (peak 22)			1253^{2+} 660 892	92–112	2505.8	Tyr
47.02 (peak 24)	43 668	3.5	659^{2+}, 1317^{+} 717^{2+}, 1432^{+} 869^{2+} 927^{2+} 985^{2+} 1057^{3+}, 1586^{2+} 821^{4+}, 1095^{3+}, 1643^{2+} 1504	91–101 91–102 76–89 or 77–90[b] 76–90[b] 76–91[b] 76–101 or 77–102 **76–102**	1316.4 1431.5 1756.1 1871.1 1986.2 3169.6 3284.6	Tyr, Phe
48.13 (peak 25)	2 586	0.2				Trp
48.87 (peak 26)	5 859	0.5	605^{2+} 927^{2+} 984^{2+} 538	103–112 76–90 76–91	1207.4 1871.1 1986.2	Tyr, Phe
55.22 (peak 34)	46 005	3.6	881^{2+}, 1763^{+} 1007	**25–39**	1762.0	Trp
55.71 (peak 35)	144 335	11.4	$688^{2+}/696^{2+}$, 1377^{+} 824^{2+} $831^{2+}/839^{2+}$ 881^{2+} $888^{2+}/896^{2+}$ 1024^{2+} 1143^{3+}, 1712^{2+} 332	10–21[b] 26–39 10–24 25–39 10–25 22–39 **10–39**	1393.5 1647.9 1678.8 1762.0 1792.9 2047.3 3422.8	Trp, Tyr
56.03 (peak 36)	52 679	4.1	824^{2+} $873^{2+}/882^{2+}$, 1763^{+} 1024^{2+}	26–39 25–39 **22–39**	1647.9 1762.0 2047.3	Trp
56.65 (peak 37)	21 352	1.7	824^{2+} 597 673 872^{2+} 947 1141^{3+}	26–39 25–39[b] 10–39	 1762.0 3422.8	Trp, Tyr
57.32 (peak 39)	47 404	3.7	460^{2+}, 918^{+} 517^{2+}, 1033^{+} $997^{2+}/1004^{2+}$ $1055^{2+}/1062^{2+}$ 755^{4+}, 1009^{3+}, 1514^{2+} 901 981	64–71 63–71 47–62 47–63 **47–71**	918.0 1033.1 2011.4 2126.4 3026.4	Tyr, Phe
58.35 (peak 40)	154 985	12.2	459^{2+}, 918^{+} 517^{2+}, 1033^{+} 951^{3+}, 1426^{2+} 990^{3+}, 1484^{2+} 1228^{3+} 971^{4+}, 1295^{3+} 901	64–71 63–71 40–62[b] 40–63[b] 42–71 **40–71**	918.0 1033.1 2870.4 2985.5 3683.3 3885.5	Tyr, Phe

TABLE I *(continued)*

Retention time (min)	Surface (220 nm)[a]	% of total surface	Masses found $(M + xH)^{x+}$	Fragments identified	(M + H), theoretical	UV Spectrum
62.24 (peak 42)	51 349	4.1	418^{+}	22–25	417.4	Tyr
			472			
			517^{2+}, 1033^{+}	63–71	1033.1	
			555			
			584			
			601			
			688^{2+}, 1376^{+}	10–21[b]	1393.5	
			719			
			745			
			793			
			831^{2+}	10–24[b]	1678.8	
			841			
			872	25–39[b]	1762.0	
			918^{+}	64–71	918.0	
			975			
			1125			
			1228			

[a] Total surface = $1301.28 \cdot 10^{-3}$ AU (220 nm) · min.

[b] These fragments arise most probably from spontaneous degradation (see text). Their masses correspond to the masses of the peptide minus 18 (loss of H_2O).

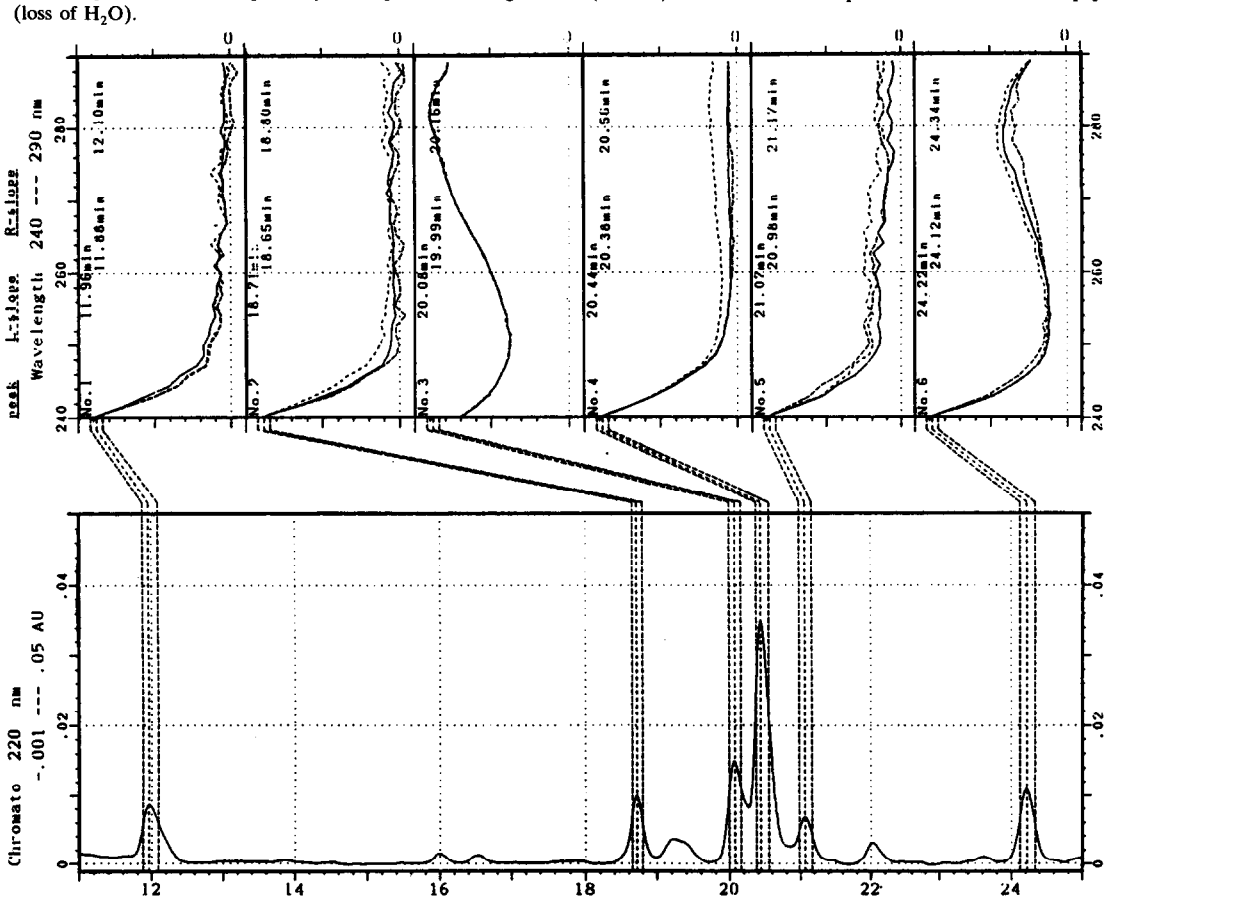

Fig. 3. Spectral analysis of the peptide map (detail). Left: expanded view of a part the chromatogram of Fig. 2. UV detection at 220 nm. Right: absorption spectra of the main peaks recorded from 240 to 290 nm.

```
                                5                                  10
MET GLN ASP / PRO TYR VAL LYS GLU // ALA GLU // ASN LEU LYS LYS
N   Q   D     P   Y   V   K   E      A   E      N   L   K   K

        15                  20                                 25
TYR PHE ASN ALA GLY HIS SER / ASP // VAL ALA / ASP // ASN GLY THR
Y   F   N   A   G   H   S     D      V   A     D      N   G   T

            30                  35                             40
LEU PHE LEU GLY ILE LEU LYS // ASN TRP LYS GLU GLU // SER ASP /
L   F   L   G   I   L   K      N   W   K   E   E      S   D

                45                  50                         55
ARG LYS ILE MET GLN //  SER GLN ILE VAL SER PHE TYR PHE LYS LEU R
K   I   M   Q       S   Q   I   V   S   F   Y   F   K   L
                    60                  65                     70
PHE LYS ASN PHE LYS ASP // ASP // GLN SER ILE GLN LYS SER VAL
F   K   N   F   K   D      D      Q   S   I   Q   K   S   V

                        75                  80
GLU // THR ILE LYS GLU // ASP / MET ASN VAL LYS PHE PHE ASN SER
E      T   I   K   E      D     M   N   V   K   F   F   N   S

85                      90                  95
ASN LYS LYS LYS ARG ASP / ASP // PHE GLU // LYS LEU THR ASN TYR
N   K   K   K   R   D     D      F   E      K   L   T   N   V

        100                 105                 110
SER VAL THR / ASP // LEU ASN VAL GLN ARG LYS ALA ILE HIS GLU //
S   V   T     D      L   N   V   Q   R   K   A   I   H   E

            115                 120                 125
LEU ILE GLN VAL MET ALA GLU //  LEU SER PRO ALA ALA LYS THR GLY L
I   Q   V   M   A   E      L   S   P   A   A   K   T   G

            130                 135                 140
LYS ARG LYS ARG SER GLN // MET LEU PHE ARG GLY ARG ARG ALA SER
K   R   K   R   S   Q      M   L   F   R   G   R   R   A   S

GLN
Q

//  peptide bonds subjected to enzymatic hydrolysis
/   peptide bonds susceptible to thermal hydrolysis.
```

Fig. 4. Observed enzymatic and thermal cleavage sites of rhIFN-γ.

apparent masses of the accompanying Na^+ and K^+ adducts, as is shown below.

Peptide fragmentation in the thermospray interface

Fragments resulting from the hydrolysis of a specific peptide bond are observed. In general, peptide bonds are acid labile. However, in dilute acid conditions, the peptide bond involving an aspartic acid is hydrolysed 100 times more rapidly than the other peptide bonds [20]. This mechanism explains certain fragmentations that occur during the thermospray injection. This phenomenon was observed after the installation of a new TSP II varporizer. We assume that the vaporizer contains a catalyst for this kind of hydrolysis or that the temperature conductance is changed, so that the sample is heated in a more efficient way. The observed thermal and/or enzymatic hydrolyses that have been observed with this interface are summarized in Fig. 4.

As an example of a mass spectrum, the spectrum of peak 21 (Fig. 2b) is given in Fig. 5. The

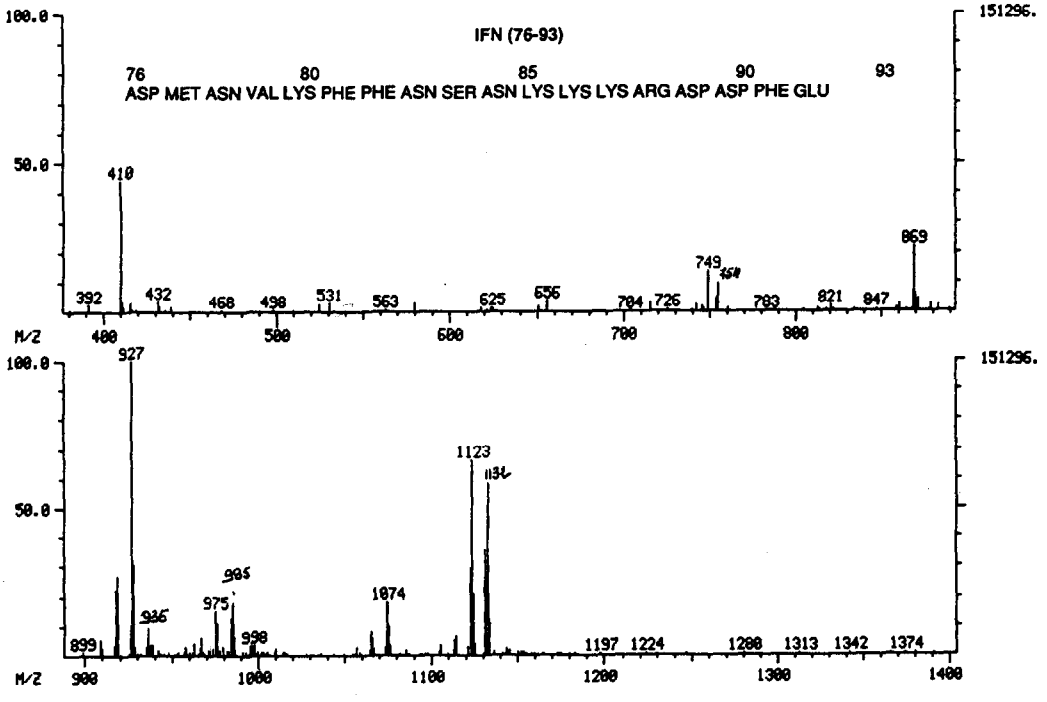

Fig. 5. Mass spectrum of peak 21 attributed to fragment IFN (76–93).

results of the analysis are given in Table I and illustrate the formation of multiply charged ions and hydrolysis of the aspartic peptide bond. The doubly charged ion from the molecular ion of peptide 76–93 (1132^{2+}) is shown in Fig. 6 and represents the 1100–1200 u region of Fig. 5. Doubly and singly charged ions from the peptides resulting from the cleavage of Asp–Met, Asp–Asp and Asp–Phe (1074^{2+}, 985^{2+}, 936^{2+}, 877^{2+}, 410^{+}) are also found.

It was not always possible to detect the singly charged parent ion for these peptides, but the apparent masses of the adducts of Na^{+} and K^{+} enabled us to assign these as multiply charged ions.

The finding of fragment 3–7 in two different peaks (6 and 8) also indicates postcolumn fragmentation. The apparent co-elution with fragment 0–2 or 0–2ox (oxidation of the methionine) must be due to the hydrolysis of the fragment IFN 0–7 after position 2 (Asp). In peak 8 the parent molecule is also found.

At the end of the peptide map, where large peptides are eluted, the presence of acid hydrolysis products enables us to retrace the parent peptide, which can be found as a series of multiply charged ions. For example, in peak 39 all hydrolysis products plus the parent molecule are observed.

Spontaneous fragmentation

Besides hydrolysis, spontaneous fragmentation can be used to explain the masses of certain fragments. Apparently this fragmentation cleaves the peptide bond, by a mechanism similar to that causing peptide bond cleavage in FAB or MS–MS ionization. It results in the loss of 18 u with respect to similar fragments obtained by hydrolysis. Consider, for example, peak 21 (Table I). The mass spectrum of this peak

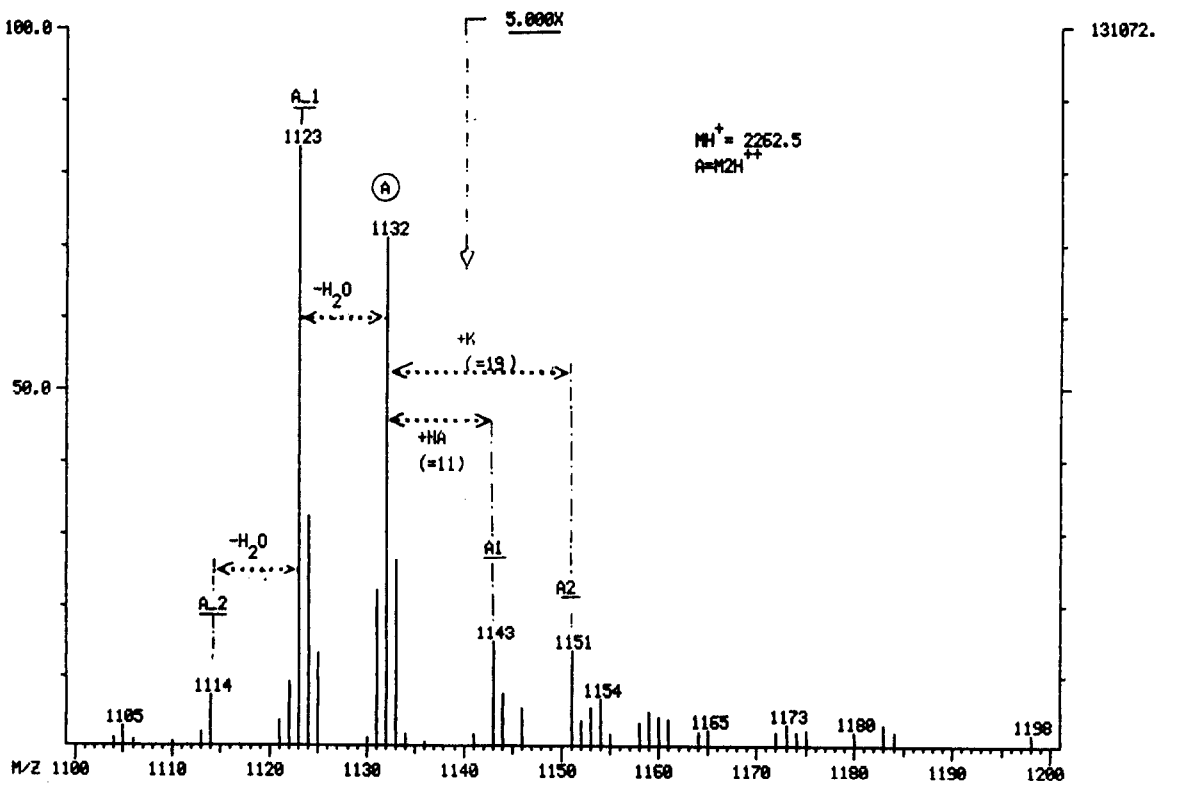

Fig. 6. 1100–1200 u region of the mass spectrum of peak 21 attributed to fragment IFN (76–93).

contains fragments due to acid hydrolysis, in addition to spontaneous fragmentation: fragment 77–90, masses $869^{2+}/877^{2+}$; fragment 76–90, masses $927^{2+}/936^{2+}$; and fragment 76–91, mass 985^{2+}.

It should also be noted that apparently abnormal cleavage sites are found, at the C-terminal side from Gln at positions 46 and 133. In these cases the complementary fragment is also found (40–46 with 47–71 and 120–133 with 134–143) elsewhere in the peptide map. The sequence around these sites, Met–Gln–Ser and Ser–Gln–Met, is remarkable. Another abnormal cleavage is found at the Lys–Asn bond (34–35).

Sensitivity

The amount of hydrolysate injected was 200 μg. We were able to determine masses in peaks that account for less than 0.2% of the total surface in the peptide map. We estimate the amount of material under this peak as 400 ng (less than 4 nmol of amino acids) (peaks 1, 2, 6, 10 and 12).

CONCLUSIONS

The peptide map of rhIFN-γ was determined by on-line RP-HPLC with diode-array absorbance and thermospray mass spectrometric detection. Fragmentation of the peptides by acid hydrolysis of the peptide bond involving aspartic acid and spontaneous fragmentation were observed. They were of great use in the identification of most of the peptides resulting from the digest of rhIFN-γ by *Staphylococcus aureus* strain V8 endoprotease. The recording of the UV absorption spectra of the fragments is of interest for the identification of the peptides and permits the extrapolation of the results to those obtained without coupling to a thermospray mass spectrometer.

REFERENCES

1 R.L. Garnick, N.J. Solli and P.A. Papa, *Anal. Chem.*, 60 (1988) 2546.
2 V.M. Ingram, *Methods Enzymol.*, 6 (1963) 831.
3 S.A. Carr, M.E. Hemling, M.F. Bean and G.D. Roberts, *Anal. Chem.*, 63 (1991) 2802.
4 Y. Ito, T. Takeuchi and D. Joto, *J. Chromatogr.*, 346 (1985) 161.
5 R.M. Caprioli, B. DaGue, T. Fan and W.T. Moore, *Biochem. Biophys. Res. Commun.*, 146 (1987) 291.
6 W.J. Henzel, J.H. Bourell and J.T. Stults, *Anal. Biochem.*, 187 (1990) 228.
7 A. Cappiello, P. Palma, I.A. Papayannopoulos and K. Biemann, *Chromatographia*, 30 (1990) 477.
8 A.P. Bruins, T.R. Covey and J.D. Henion, *Anal. Chem.*, 59 (1987) 2642.
9 E.C. Huang and J.D. Henion, *Anal. Chem.*, 63 (1991) 732.
10 C.R. Blakey, J.J. Carmody and M.L. Vestal, *Anal. Chem.*, 52 (1980) 1636.
11 H.Y. Kim, D. Pilosof, D.F. Dyckes and M.L. Vestal, *J. Am. Chem. Soc.*, 106 (1984) 7304.
12 D. Pilosof, H.Y. Kim, D.F. Dyckes and M.L. Vestal, *Anal. Chem.*, 56 (1984) 1236.
13 W.P. Blackstock, R.J. Dennis, S.J. Lane, J.I. Sparks and M.P. Weir, *Anal. Biochem.*, 175 (1988) 319.
14 P.J. Rudewicz, *Biomed. Environ. Mass Spectrom.*, 15 (1988) 461.
15 K. Stachowiak, C. Wilder, M.L. Vestal and D.F. Dyckes, *J. Am. Chem. Soc.*, 110 (1988) 1758.
16 K. Stachowiak and D.F. Dyckes, *Pept. Res.*, 2 (1989) 267.
17 K. Straub and K. Chan, *Rapid Commun. Mass Spectrom.*, 4 (1990) 267.
18 K. Chan, D. Wintergrass and K. Straub, *Rapid Commun. Mass Spectrom.*, 4 (1990) 139.
19 R.H. Robins and F.W. Crow, *Rapid Commun. Mass Spectrom.*, 2 (1988) 30.
20 C.M. Tsung and H. Fraenkel-Conrat, *Biochemistry*, 4 (1965) 793.